Supplementary data

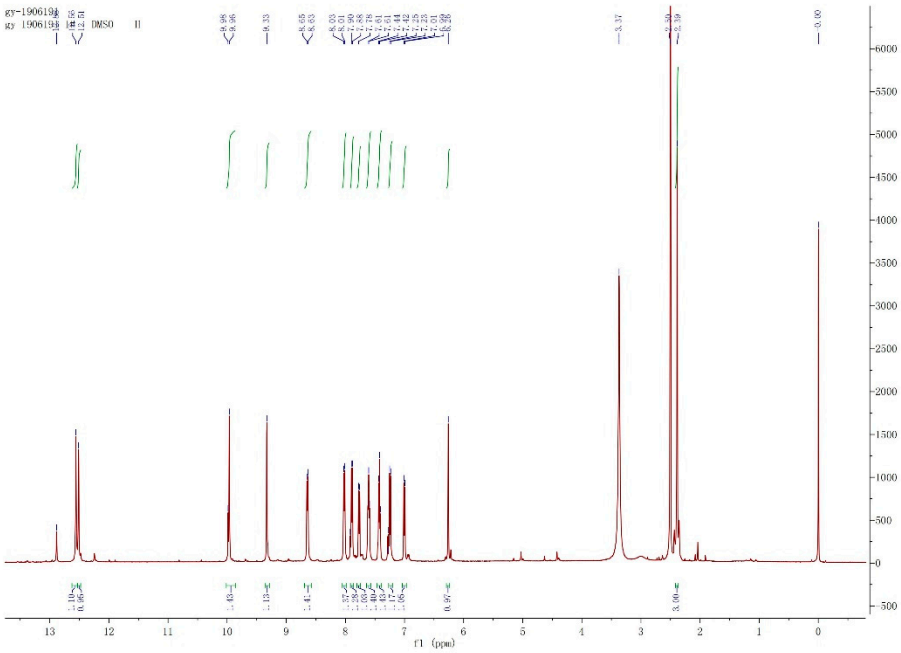

Figure S1. ^{1}H NMR of **NL** (DMSO-*d*6).

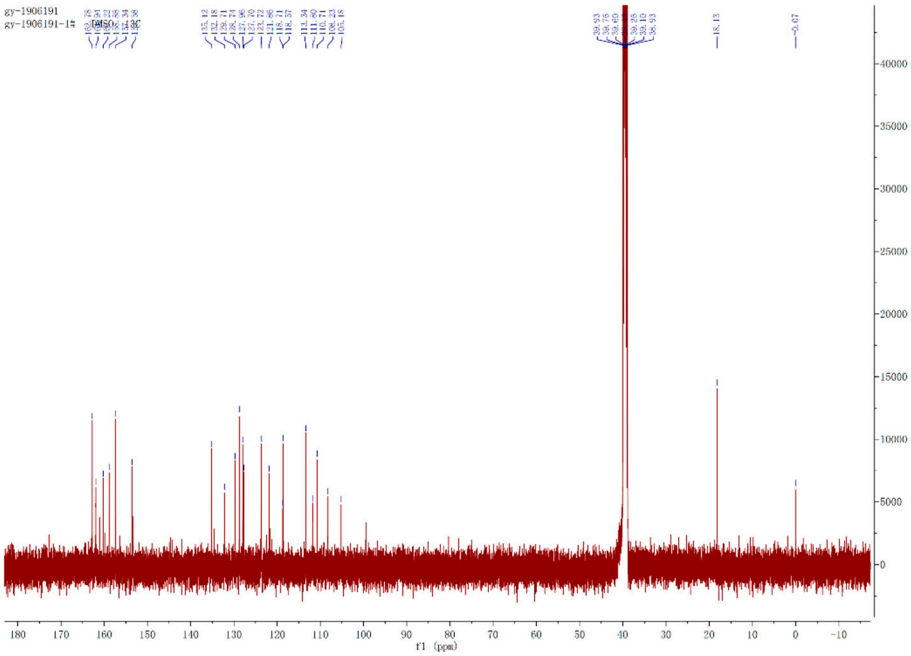

Figure S2. ^{13}C NMR of **NL** (DMSO-*d*6).

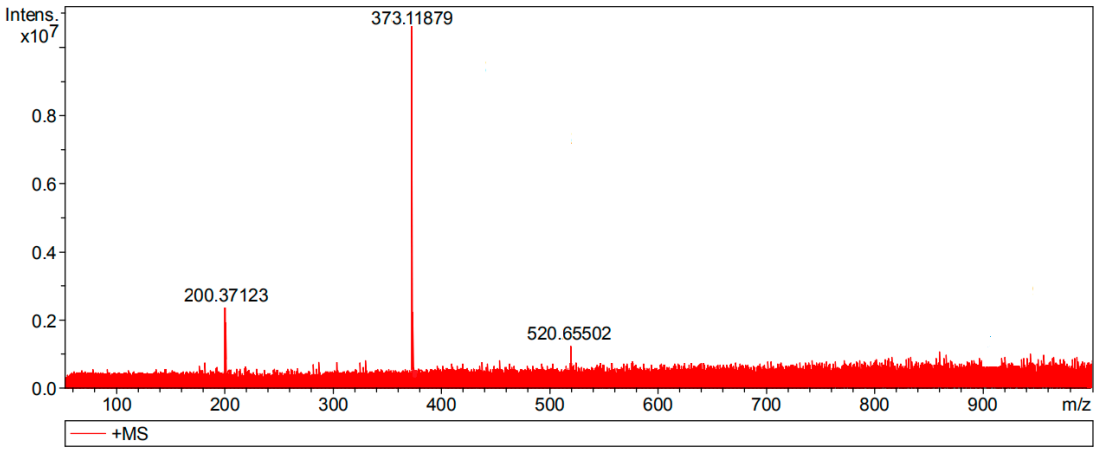

Figure S3. FT-MS of NL .

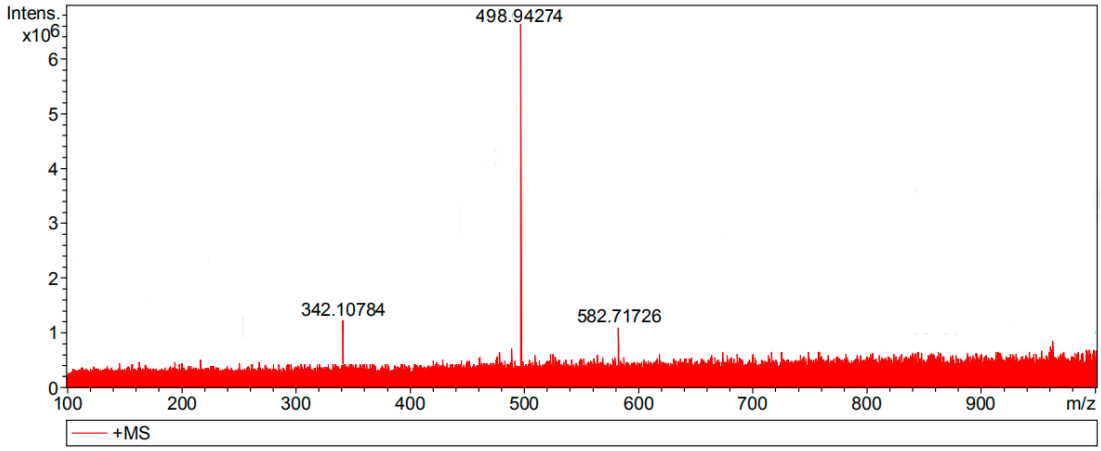

Figure S4. FT-MS of **NL**-Fe^{3+} complex.

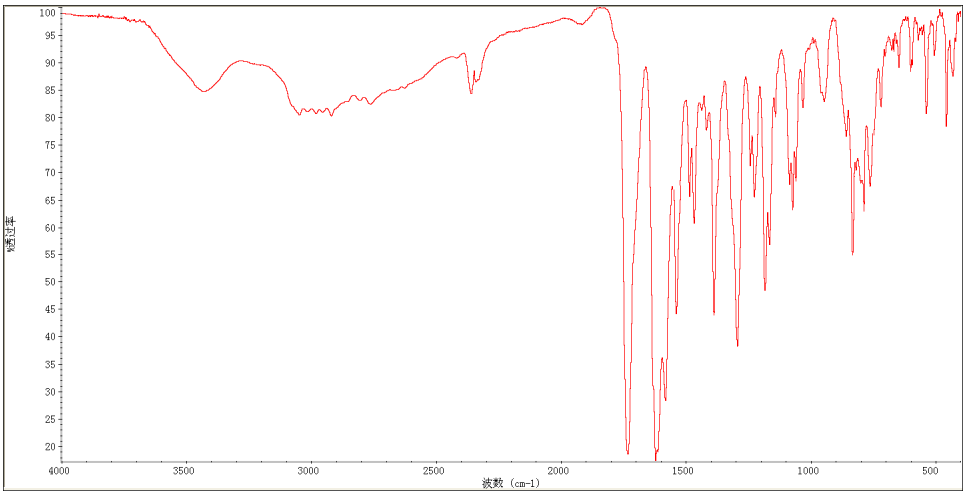

Figure S5. IR of **NL**-Fe^{3+} complex **.**

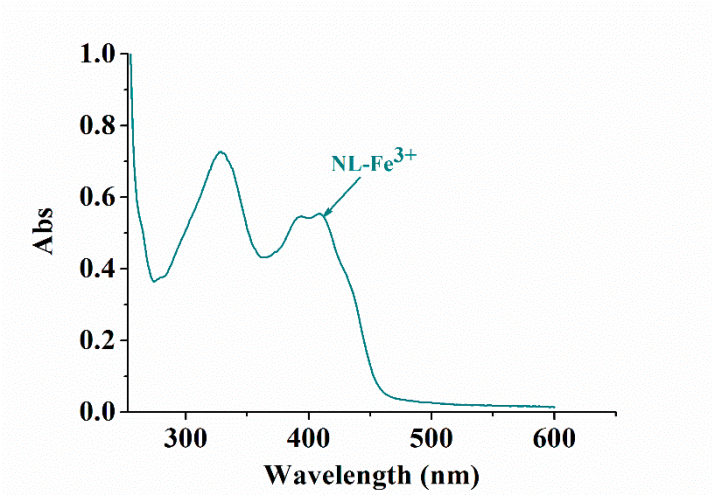

Figure S6. UV-Vis of **NL**-Fe^{3+} complex **.**

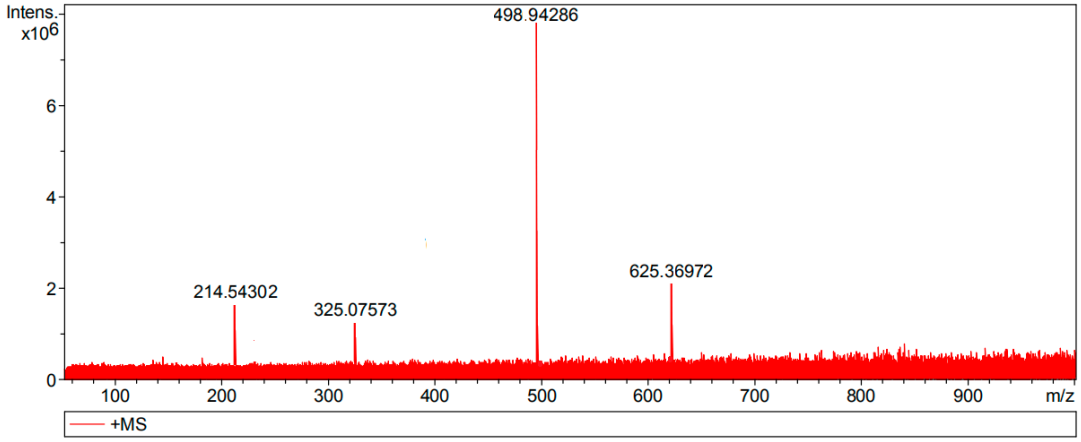

Figure S7. FT-MS by adding Fe^{3+} into **NL .**

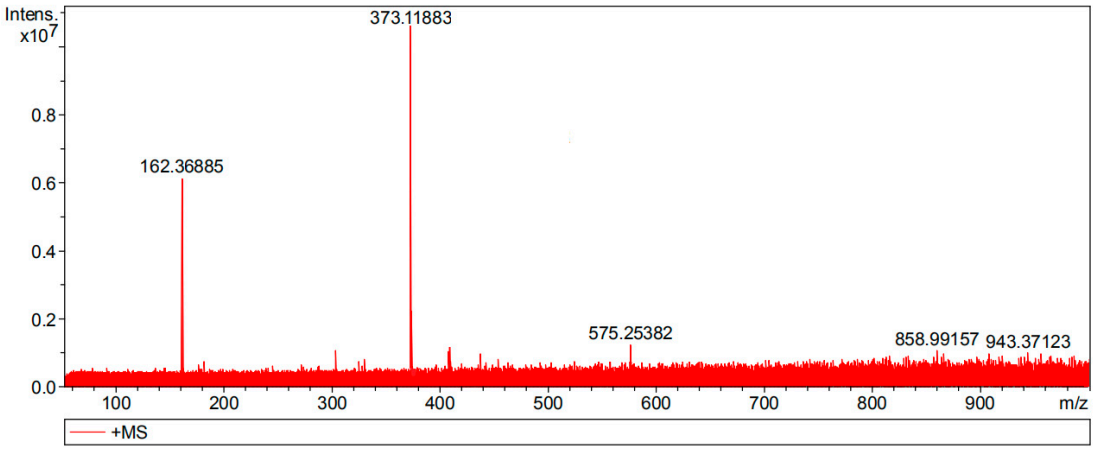

Figure S8. FT-MS of **NL**-Fe^{3+}+PPi .

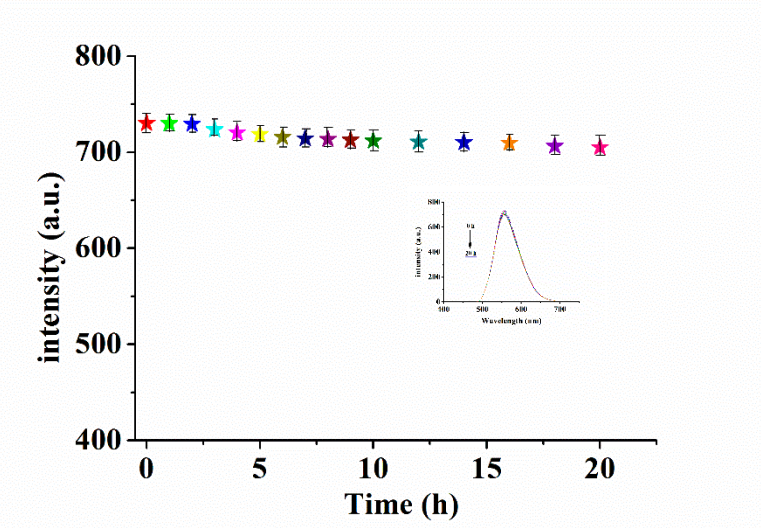

Figure S9. Fluorescence spectra of **NL** (10 μM) at different times in DMSO/H_2O (2:8/v:v, 20 mM HEPES, pH=7.2) solutions (*λex*=410nm).

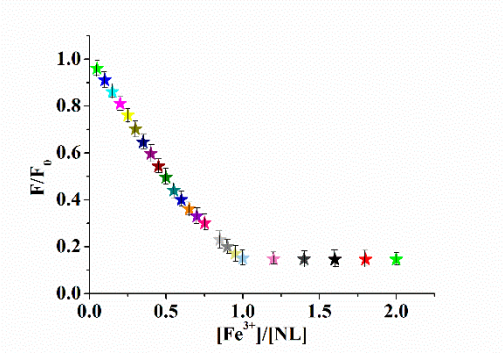

Figure S10. Fluorescence intensities of **NL** (10 μM) at 557nm as a function of Fe^{3+} concentration (0-20 μM) in DMSO/H_2O (2:8/v:v, 20 mM HEPES,, pH=7.2) solutions (*λex*=410 nm).

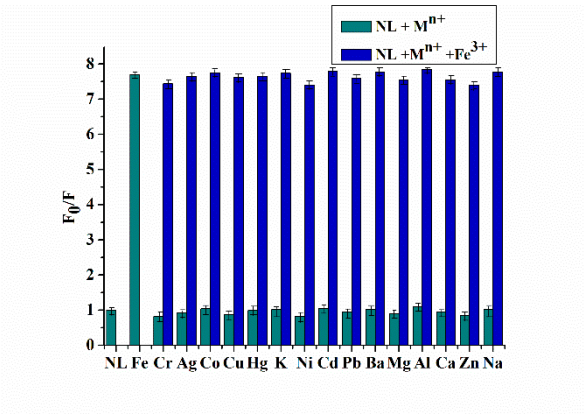

Figure S11. Fluorescence response of **NL** (10 μM) to Fe^{3+} (20 μM) in the presence of other common metal ions (20 μM). The green bars represent the enhancement degree of **NL** in the presence of cations of interest (all are 20 μM). The blue bars represent the changes of the emission that occurs upon the subsequent addition of Fe^{3+} (20 μM) to the above solution (*λex*=410 nm).

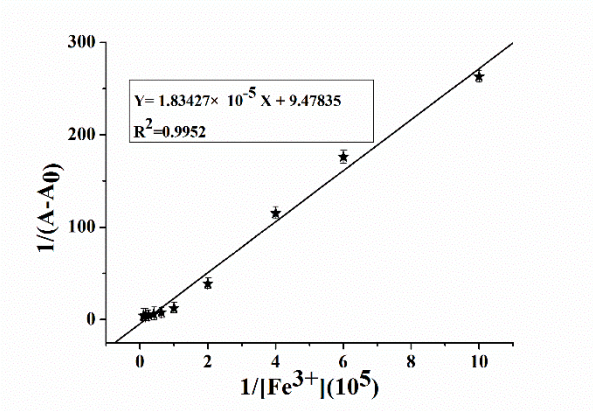

Figure S12. The Benesi-Hildebrand plot of **NL**(10 μM) with Fe^{3+}(20 μM) by UV-Vis spectroscopy.

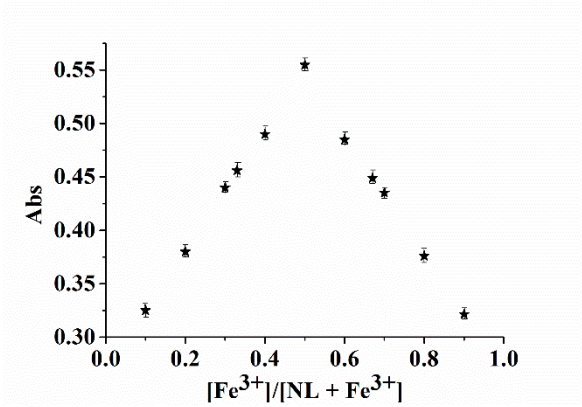

Figure S13. The Job's plot of the reaction between **NL** and Fe^{3+} by UV-Vis spectroscopy.

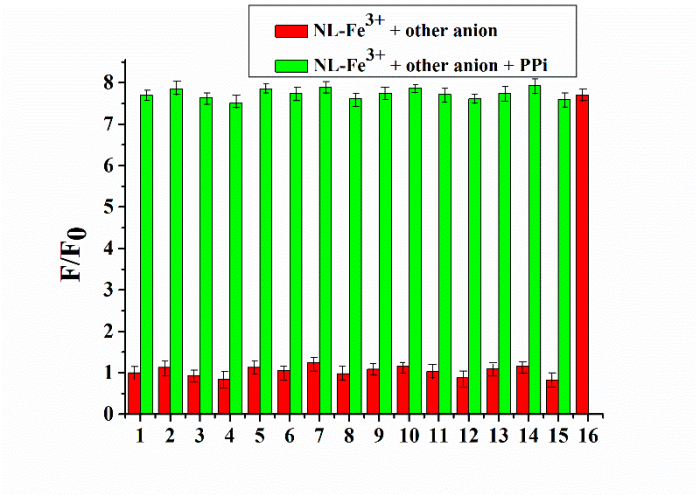

Figure S14. Fluorescence response of **NL**-Fe^{3+} (10 μM) in the presence of various analytes (40 μM): (1) NO_2^-, (2) S^{2-}, (3) F^-, (4) SCN^-, (5) Ac^-, (6) HCO_3^-, (7) HSO_4^-, (8) CO_3^{2-}, (9) Cl^-, (10) Br^-, (11) SO_4^{2-}, (12) AMP, (13) ADP, (14) ATP, (15) Pi, (16) PPi (λex=410 nm).

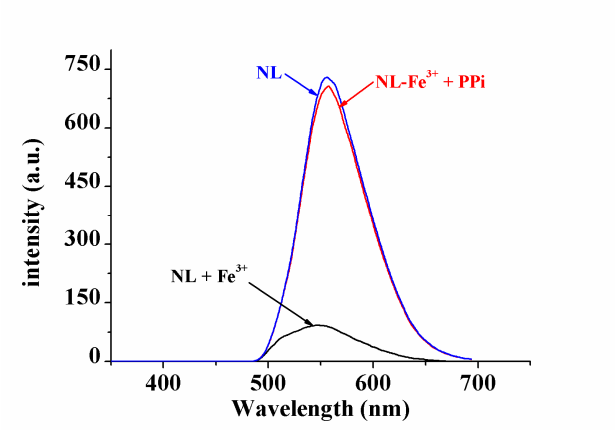

Figure S15. Fluorescence spectra of **NL** (10 μM), sequential upon addition of Fe^{3+} (20 μM) and PPi (40 μM) in DMSO/H_2O (2:8/v:v, 20 mM HEPES, pH=7.2) solutions(λex=410 nm).

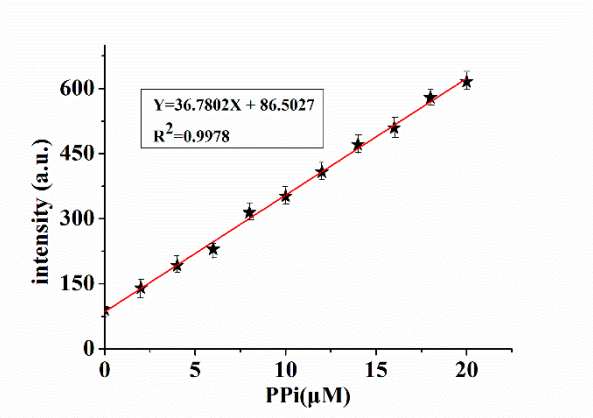

Figure S16. The linear responses of **NL**-Fe^{3+} (10 μM) versus the concentration of PPi (0-20 μM) in DMSO/H_2O (2:8/v:v, 20 mM HEPES, pH=7.2) solutions.

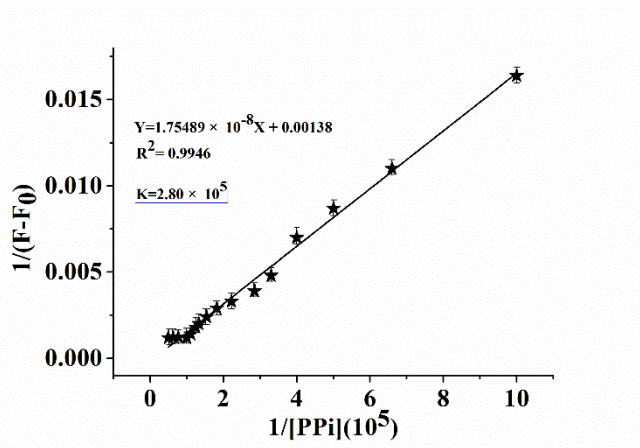

Figure S17. The decomplexation constant of **NL**-Fe^{3+} toward PPi by fluorescence titration.

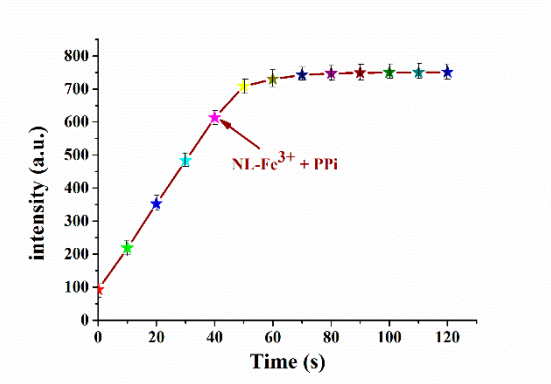

Figure S18. The fluorescence response time of **NL**-Fe^{3+} (10 μM) in the presence of PPi (40 μM) in DMSO/H_2O (2:8/v:v, 20 mM HEPES, pH=7.2) solutions.

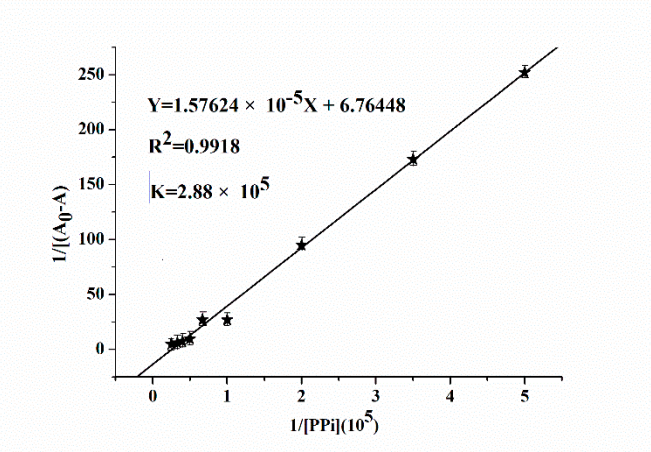

Figure S19. The decomplexation constant of **NL**-Fe^{3+} toward PPi by UV-Vis spectroscopy.

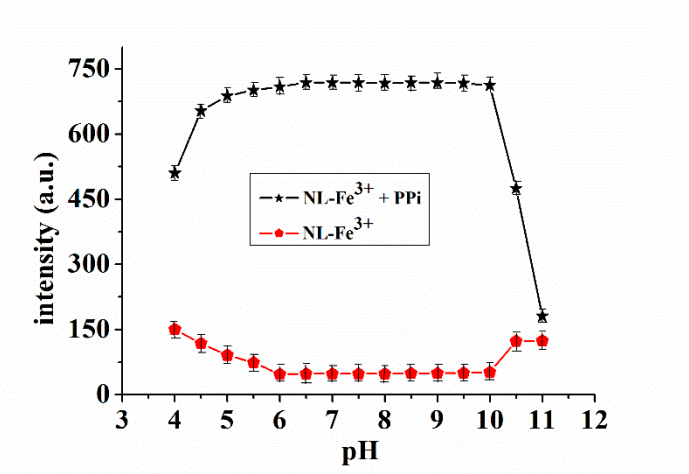

Figure S20. Fluorescence intensity of **NL**-Fe^{3+} (10 μM) in the absence and presence of PPi (40 μM) ion at various pH values in DMSO/H_2O (2:8/v:v, 20 mM HEPES, pH=7.2) solutions.

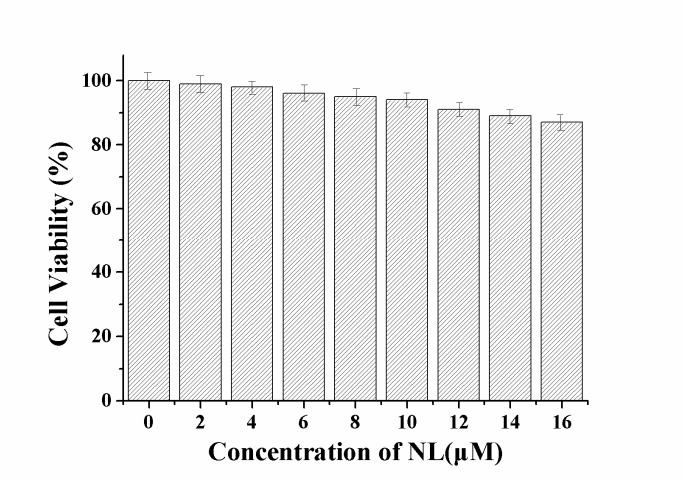

Figure S21. Cell viability values (%) assessed using an MTT proliferation test versus incubation concentrations of **NL**. Hep G2 cells were cultured in the presence of **NL** (2-16 μM) at 25 °C for 24 h. Viability(%) = mean of absorbance value of treatment group/mean absorbance value of control × 100%.

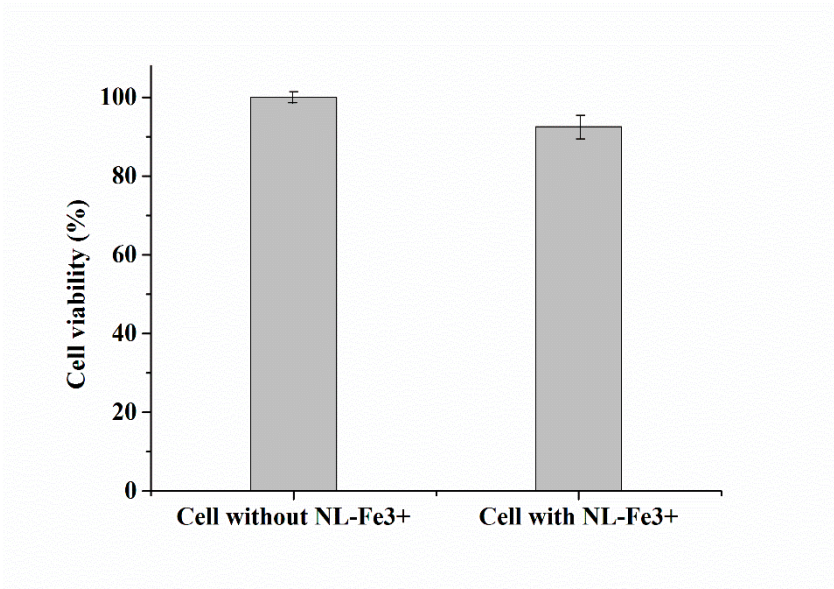

Figure S22. MTT assay of Hep G2 cells treated with **NL**-Fe^{3+} (10 μM) .